Super-Solidus Hot Isostatic Pressing Heat Treatments for Advanced Single Crystal Ni-Base Superalloys

INMACULADA LOPEZ-GALILEA, LISA HECKER, ALEXANDER EPISHIN, DAVID BÜRGER, BENJAMIN RUTTERT, PASCAL THOME, SEBASTIAN WEBER, and WERNER THEISEN

Super-solidus hot isostatic pressing (SSHIP) heat treatment has first been developed and applied to the third-generation Ni-base single crystal superalloy CMSX-10 K. This new type of heat treatment aims at significantly reducing the total time required for the solution heat treatment and at enhancing mechanical properties as compared to conventional heat treatment routes. The SSHIP is an innovative, economical and sustainable approach that can be applied to all types of Ni-base SX superalloys. It is especially interesting for alloys with a high content of refractory elements and a large volume fraction of eutectic microstructure in the as-cast state.

https://doi.org/10.1007/s11661-022-06884-y

I. INTRODUCTION

THE amount of refractory elements in advanced single crystal (SX) Ni-base superalloys has steadily increased throughout the last decades,[1] enhancing creep resistance due to improved solid solution strengthening, increasing γ'-phase stability and lowering diffusion rates.[2] Unfortunately, in most cases these alloys require long and expensive homogenization-solution heat treatments at high temperatures ($T_{\gamma'\text{-solvus}} < T < T_{\text{solidus}}$) in order to reduce large scale chemical heterogeneities within the dendritic structure and to prevent undesired microstructural features like high amounts of γ/γ' eutectics and topologically close-packed (TCP) phases, formed during solidification.

The most challenging aspect in designing homogenization-solution heat treatments is the need to avoid incipient melting associated with low local solidus temperatures in eutectic parts of the as-cast microstructure.[3,4] The great difficulty in accurately identifying γ'-solvus and solidus temperatures, due to the broad and smeared out endothermic and exothermic peaks recorded using differential scanning calorimetry (DSC), makes it a real challenge to design homogenization-solution heat treatments for superalloys.[5] Moreover, phase transformation temperatures may vary with heating and cooling rates, as well as with the degree of homogenization.[4] Accordingly, the conventional homogenization-solution heat treatment is a multi-step process, where starting at temperatures below the melting point of the eutectic regions, the material is exposed to subsequent annealing steps during which diffusion processes between dendritic and interdendritic regions result in chemical homogenization and, as a result, in a stepwise increase of the melting point of the interdendritic regions. This can lead to extended homogenization-solution heat treatments that can be difficult to control.[4] In addition, the time and energy to homogenize-solution these alloys have increased as more and more refractory elements have been added. These tedious heat treatments increase the costs associated with processing.[6] As an example, the third-generation single crystal CMSX-10, which contains a 6 wt pct in Re, requires 10 heating steps, which take a total time of about 45 hours and reach temperatures of up to 1365 °C during solution heat treatment.[1,7]

Another (negative) side effect of these required long heat treatments is the increase of porosity associated with different solid-state diffusion processes, including decrease of hydrostatic tensile stresses in dendritic regions, growth of pores between secondary dendrite arms and the Kirkendall effect. An increased porosity results in a significant reduction of mechanical properties including a decrease of creep ductility and a decrease

INMACULADA LOPEZ-GALILEA, LISA HECKER, DAVID BÜRGER, BENJAMIN RUTTERT, PASCAL THOME, SEBASTIAN WEBER and WERNER THEISEN are with the Institute for Materials, Ruhr-Universität Bochum, Universitätsstr. 150, 44801 Bochum, Germany. Contact: lopez@wtech.rub.de ALEXANDER EPISHIN is with the Merzhanov Institute of Structural Macrokinetics and Materials Science, Russian Academy of Sciences (ISMAN), Chernogolovka, Russia, 142432.
Manuscript submitted July 14, 2022; accepted October 25, 2022.
Article published online November 23, 2022

of fatigue life.[8–14] One efficient way to reduce the porosity significantly is by hot isostatic pressing (HIP).[15–17] However, HIP needs to be performed at high temperature close to the solidus-temperature and carries the risk of recrystallization and incipient melting.[18,19] Modern HIP facilities allow to work with rapid cooling rates (quenching) and to combine the homogenization-solution heat treatment and the HIP heat treatment into one single step.[16] The use of this type of facility at temperatures between γ'-solvus and solidus has shown great potential with regard to the simultaneous reduction of porosity and segregation.[9,10,12,13,16]

Homogenization-solution heat treatments or HIP heat treatments of SX Ni-base superalloys carried out at super-solidus temperatures are rare to find or do not exist, due to the fact that incipient melting in SX Ni-base superalloys has been completely avoided until now. However, this kind of heat treatment is called Super-solidus Liquid Phase Sintering (SLPS) or solely Liquid Phase Sintering (LPS) in the literature and is very popular for other kind of Ni-base superalloys, other metal alloys and mainly for the densification of metal powders.[20–23]

In the case of a super-solidus heat treatment of SX Ni-base superalloys, it is expected that the residual interdendritic eutectics partially melt while the dendritic γ' dissolves completely. Under these conditions, diffusion in solid-state and diffusion in liquid would be observed. Due to the higher applied temperature, solid state diffusion would be faster than in conventional homogenization-solution heat treatments. On the other hand, diffusion in the liquid state is orders of magnitudes faster as compared to solid-state diffusion and therefore, the application of a super-solidus heat treatment may well reduce the total homogenization time. However, it must be considered that the formation of a liquid phase can result in the generation of new porosity associated with swelling and liquid shrinkage.

This work aims at understanding the effect of *super-solidus liquid phase heat treatments under vacuum* and *under isostatic pressure* on the microstructure and mechanical properties of the third generation CMSX-10 K Ni-base superalloy. In the present work the *super-solidus hot isostatic pressing* (SSHIP) heat treatment is considered for the first time for a SX Ni-base superalloy. This new and innovative type of heat treatment aims at significantly reducing the total homogenization-solution time and to enhance mechanical properties regarding those obtained by conventional heat treatment routes. During the application of SSHIP, a partial melting of the eutectic microstructure takes place while diffusion accelerates due to the higher temperature used. The derived swelling, due to liquid formation and the associated generation of new porosity during the cooling and resolidification stage of the material, is prevented due to the simultaneous application of isostatic pressure. The adequate control of the SSHIP parameters allows to preserve the integrity of the SX, avoiding nucleation of new grains during re-solidification. In this paper first laboratory scale results are presented.

II. MATERIAL, HEAT TREATMENTS AND EXPERIMENTAL TECHNIQUES

A. *Material*

The effect of super-solidus heat treatments has been investigated on the SX Ni-base superalloy of the third-generation CMSX-10 K casted by Howmet Alcoa, which contains a high level of refractory elements (W, Re, Mo and Ta), ~ 19 wt pct. The chemical composition of the used SX material is listed in Table I. The cast plate slab has the dimensions 175 × 100 × 20 mm, with the preferred direction of solidification of the single crystal, <001> , aligned with the largest dimension of the plate.

Cuboids with dimensions 10 × 10 × 20 mm were machined by electrical discharge machining to proceed with the super-solidus heat treatment study, while larger specimens were machined to proceed with the mechanical testing.

B. *Characterization of Phase Transformation Temperatures*

The characterization of the phase transformation temperatures has been carried out using the CALPHAD (*CALculation of PHAse Diagrams*) method and experimentally using DSC.

The Scheil-Gulliver equation, which considers no back diffusion occurring in the solid and complete mixing of the liquid phase, was used to determine the predicted phases and segregation level in the as-cast condition. The calculated values were compared and contrasted with those obtained from the experimental microstructural characterization of the material in the as-cast condition. The phase transformation temperatures, as well as the evolution of the amounts of phases and their compositions with temperature, were calculated under equilibrium conditions. These calculations were used to select the conditions for the isothermal heat treatments at super-solidus temperature. To carry out the above calculations, the specific TCNi10 database for Ni-base superalloys was considered.

Experimentally, in order to evaluate the transition temperatures of the main phases that appear in the as-cast SX material as well as after the different isothermal heat treatments studied, DSC was used. Because the specimens for the DSC test must represent the microstructure of the different conditions studied and considering the strong segregation present in the cast materials and their high-density values, specimens with a weight of about 50 mg were used. The tests were performed in a high purity helium purged atmosphere

Table I. Chemical Composition (in Wt Pct) of the CMSX-10 K Material

Ni	Cr	Mo	Co	W	Re	Al	Ti	Ta	Hf	Nb
Bal	2	0.4	3	5	6	5.7	0.2	8	0.03	0.1

Table II. Heat Treatments Carried Out at Super-Solidus Temperatures

Name	Furnace type	Temperature [°C]	Total holding time [hours]
V-1365 °C-1 hour	vacuum	1365	1
V-1365 °C-4 hours			4
HIP-1365 °C-4 hours	HIP	1365	4
HIP-1370 °C-4 hours		1370	4
SSHIP		1365/1370	10

The temperature values indicate the temperature of the different holding steps carried out in each heat treatment.

and consisted of a heating ramp at a constant rate of 20 °C/min from RT to 1500 °C, followed by a cooling ramp at 20 °C/min to RT. To obtain reliable results, duplicate samples were evaluated for each study condition.

C. *Heat Treatments*

To develop the SSHIP heat treatment, different thermal treatments at super-solidus temperatures were carried out using a Schmetz vacuum furnace, as well as a Quintus QIH-9 HIP-Quench-unit. Due to the strong amount of segregation introduced during casting, the eutectic regions are considered to be the areas with the lowest melting temperature and therefore those that set the guidelines for heat treatments. Isothermal heat treatments were carried out at temperatures slightly above the incipient melting temperature for CMSX-10 K for different holding times. Table II presents an overview of the heat treatments carried out in this work. The first type of isothermal heat treatment was carried out in the vacuum furnace at 1365 °C, where the specimens were kept for 1 hour or 4 hours at the maximum temperature and then quenched directly after heat treatment by using 5 bar of N_2. These heat treatments were named V-1365 °C-1 hour and V-1365 °C-4 hours respectively. The second type of heat treatment was carried out in a HIP-Quench-unit, using a maximum temperature of 1365 °C and 1370 °C for 4 hours of holding time with a rapid cooling to room temperature (RT). These heat treatments were named HIP-1365 °C-4 hours and HIP-1370 °C-4 hours, respectively. A heating ramp of 20 °C/min was selected to heat the specimens up to the maximum temperature applied in each of the isothermal heat treatments. The fast cooling option was selected for all heat treatments to freeze the microstructure developed at high temperature and track microstructural evolution during the proposed heat treatments. Finally, a super-solidus hot isostatic pressing heat treatment was performed, consisting of a heating ramp of 20 °C/min and two isothermal stages, both at super-solidus temperatures. The two isothermal stages consist of 4 hours at 1365 °C and 6 hours at 1370 °C, after which the specimens were quenched to obtain a fine and homogeneous distribution of the γ/γ' microstructure. This new type of heat treatment was briefly referred to as SSHIP in Table II. The SSHIP heat treatment aims to replace tedious and lengthy conventional solution annealing heat treatments that have total holding times of up to 45 hours.[1,7,24–26] For mechanical testing purposes, SSHIP specimens were subjected to the standard aging heat treatment described in Refs. 7 and 25. The optimization of the aging heat treatment is outside the scope of this manuscript.

D. *Metallographic Preparation*

As-cast and heat-treated specimens were prepared metallographically for microstructural characterization. Cross-sections of the specimens, perpendicular to the <001> direction, were embedded in a conductive resin, ground, and polished with diamond suspension to 1 μm. The specimens were then vibropolished for at least 2 hours. This type of sample preparation is required for Energy-Dispersive X-ray diffraction (EDX) and Electron Backscatter Diffraction (EBSD). To achieve topographic contrast in the secondary electron (SE) mode, γ'-precipitates are etched by immersing the specimens in a mixture of 40 ml deionized water, 20 ml HCl and 10 ml H_2O_2 at room temperature for 3–4 seconds.

E. *Microstructural Characterization*

The characterization of the microstructure of the study material in as-cast condition, after different isothermal heat treatments as well as after mechanical testing was carried out using the LEO 1530 VP (ZEISS) scanning electron microscope (SEM), operating at 21 kV. The secondary electron (SE) and backscattered electron (BSE) imaging modes were used.

The quantification of microstructural defects such as porosity, eutectics and incipient melting was performed by stage scans at the SEM, where about 154 SEM images were taken at a magnification of 500 times, covering a representative area of at least 4 mm^2.

Furthermore, the degree of homogenization of the composition achieved after the different heat treatments was measured using Energy-Dispersive X-ray diffraction (EDX) at the LEO SEM. For this purpose, line scans between the regions of interest, dendrite core (DC) and interdendritic region (ID), as well as composition maps covering specific regions were carried out.

The characterization of the crystallographic orientation of the new re-solidified regions after incipient melting, was done by performing electron backscatter diffraction (EBSD) at the MIRA SEM microscope operating with a voltage of 20 kV, a working distance of 15 mm and an inclination of the samples of 60 deg.

The scanning step of 0.2 μm was chosen to obtain good quality results.

In addition to the standard EBSD characterization a high resolution EBSD method (Rotation-Vector-Baseline-EBSD, RVB-EBSD[27]) was used to quantify slight misorientations around pores in the re-solidified regions. The RVB-EBSD method was originally developed to characterize small misorientations between dendrites and has been successfully applied to study crystal mosaicity.[28,29] The RVB-EBSD scans were performed using a SEM of type QUANTA 650 from FEI, equipped with a field emission gun. During the EBSD measurements, the specimens were tilted to 70 deg and an acceleration voltage of 30 kV was used. The working distance was set to 17 mm and a step size of 0.5 μm was used. Kikuchi Patterns were captured using a Hikari XP camera from EDAX Inc with a 1 × 1 binning. The RVB-EBSD data was analysed with the free MATLAB[30] toolbox MTEX.[31,32]

F. *Mechanical Characterization: Creep*

To investigate the influence of applying *super-solidus liquid phase heat treatments under isostatic pressure* on the mechanical properties, uniaxial tensile creep experiments were performed on specimens heat-treated under the developed SSHIP heat treatment.

Table III. Quantitative Metallography of the Main Microstructural Heterogeneities Found in the As-Cast CMSX-10 K Alloy and in the Specimens Subjected to the Different Super-Solidus Heat Treatments

Name	Cast–Eutectic	Porosity	Re-solidified regions
As-cast	22.1	0.10	—
V-1365 °C-1 hour	1.89	0.21	2.13
V-1365 °C-4 hours	0.16	0.27	1.31
HIP-1365 °C-4 hours	5	~ 0	0
HIP-1370 °C-4 hours	0	0.05	0.20
SSHIP	< 0.1	< 0.002	0

Values in area pct.

The creep behaviour of the materials resulting from the SSHIP heat treatment were studied by performing miniature creep tests on tensile specimens oriented in the <001> direction. The miniature creep test technique and all aspects concerning the creep data acquisition from uniaxial tensile specimens are described by Wollgram *et al.*[33] Due to the fact that the selected alloy is considered to operate at high temperature, the following creep conditions were used: temperature of 1050 °C and stress level of 170 MPa. On the other hand, these conditions were selected in order to compare them with reported CMSX-10 K creep results from Portella *et al.* (DFG project number: 5193782).[34]

III. RESULTS

A. *As-Cast CMSX-10 K Material*

The characterization of the microstructure of the CMSX-10 K alloy in the as-cast state allows establishing the appropriate temperatures for super-solidus heat treatments. This characterization has been done experimentally and through the support of thermodynamic calculations.

The as-cast material shows a highly segregated dendritic structure (dendrite growth direction <001>) with a high amount of eutectic regions, ~ 22 area pct, and a porosity around 0.1 area pct (Table III). The chemical compositions measured in the DC, ID and eutectic regions by EDX reveal a high concentration of Re and W in the DC and a high concentration of the γ'-forming elements, Al, Ti and Ta in the ID and eutectics, being higher in the eutectic regions (Table IV). Figure 1 shows representative images of the γ/γ' at DC (a) and ID (b) as well as images of the eutectic regions and as-cast porosity (c and d). In DC, the material presents a finer γ/γ' microstructure compared to that observed at the ID. Almost all of the pores are in direct contact with the eutectic zones.

The melting temperature associated with incipient melting of the eutectic regions was measured by DSC. The obtained DSC heating curve for the as-cast material shows two endothermic peaks [solid line in Figure 2(a)]. The first small peak that indicates the melting of eutectic regions at a value of 1361 °C is followed by a larger peak that indicates the melting of the primary dendritic structure. The value obtained for the incipient melting temperature is only around 1 °C lower than the value published by Pang *et al.*[24] for the same SX superalloy

Table IV. Chemical Compositions Measured at Different Regions of Interest, DC, ID and Eutectics, in the As-Cast Material and in the SSHIP Material

Material	Region	Ni	Cr	Mo	Co	W	Re	Al	Ti	Ta
As-cast	DC	bal	2.4	0.4	3.5	8.1	10.4	4.8	0.2	7.8
	ID	bal	1.6	0.5	2.7	3.1	1.6	7.4	0.4	14.8
	eutectic	bal	1.5	0.5	2.6	2.8	1.2	7.7	0.5	15.3
SSHIP	DC	bal	2.3	0.5	3.4	5.4	7.6	5.8	0.3	10.3
	ID	bal	2.3	0.5	3.4	4.1	5.0	6.3	0.4	11.0

Composition values in wt pct. The elements Hf and Nb have not been considered due to the limitation of the EDX detector and their low quantity in the nominal composition of the material (Table I).

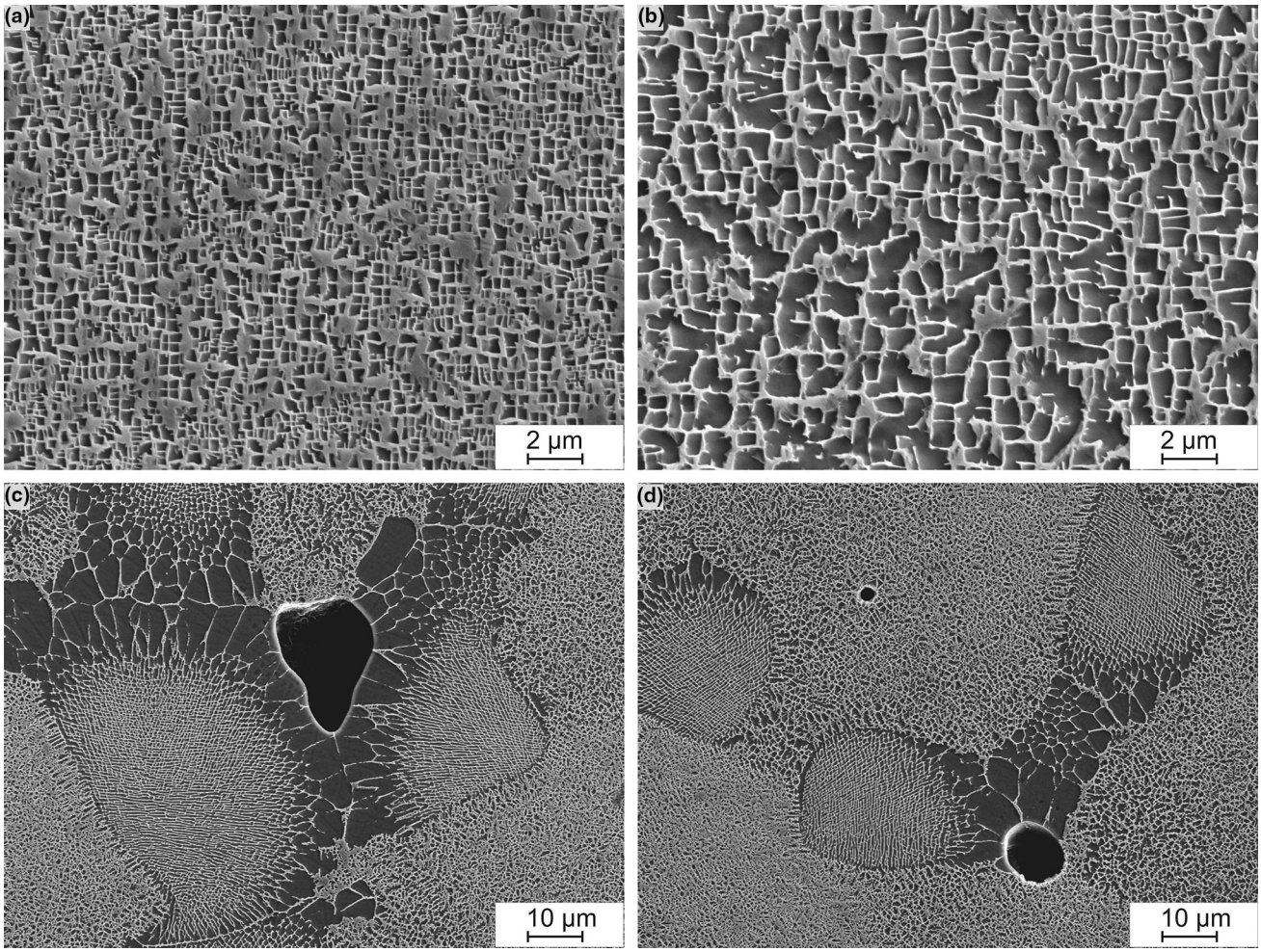

Fig. 1—Microstructure of the SX CMSX-10 K superalloy in as-cast state: (*a*) γ/γ' microstructure at the dendrite core; (*b*) γ/γ' microstructure at the interdendritic regions; (*c*) and (*d*) eutectics and porosity at the interdendritic regions.

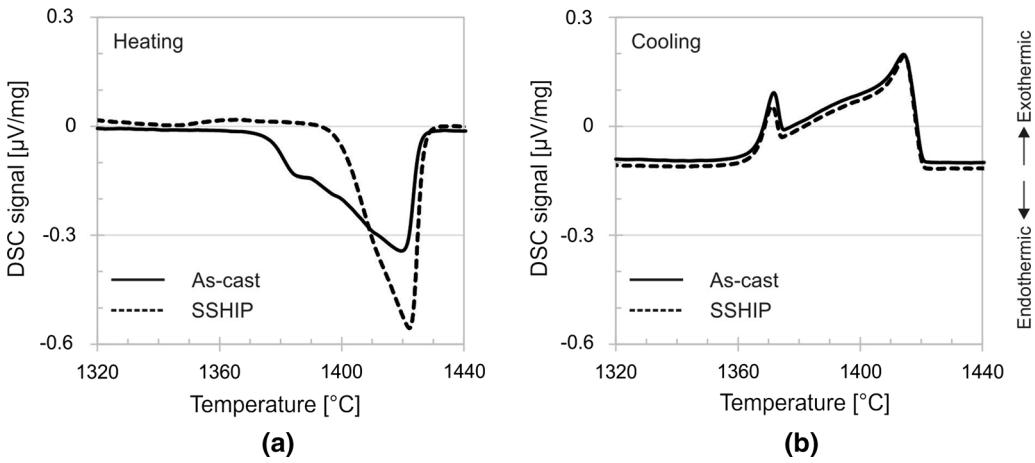

Fig. 2—DSC heating curves (*a*) and DSC cooling curves (*b*) for the as-cast material (solid lines) and the SSHIP material (dashed lines).

(Table V). From the DSC cooling curve for the as-cast material [solid line in Figure 2(b)], the value of the liquidus temperature can be deduced, which is 1421 °C.

Figure 3(a) represents the evolution of the amount of phases as a function of the temperature during Scheil solidification and the corresponding main transformation temperatures of the phases are listed in Table V.

Table V. Phase Transformation Temperatures for CMSX-10 K Measured by Different Techniques

	Thermo-Calc® Equilibrium	Thermo-Calc® Scheil	DSC (Fig. 2)	DSC[24]
Liquidus	1438.4	1438.4	~ 1421	—
Solidus	1391.5	1313.4 (*)	~ 1389	1378
Eutectic Melting	—	—	~ 1361 (As-cast)	1362
γ'-solvus	1369.3	1379.4	1344–1367	—

Temperature values in °C. (*Solidus temperature calculated in the presence of 1 vol pct of liquid). Phase transformation temperature values published by Pang *et al.*[24] are listed for comparison purposes.

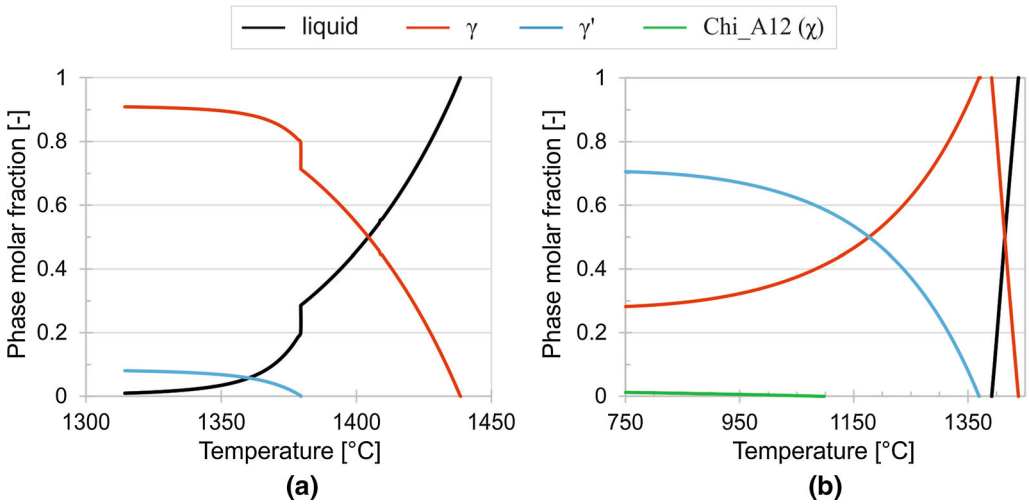

Fig. 3—(*a*) Scheil-solidification and (*b*) equilibrium calculations- property diagram for the nominal composition (Color figure online).

According to Scheil, the precipitation of γ' is calculated at the end of the solidification, at temperatures below 1379.4 °C and reaches a maximum phase fraction of ~ 8 pct at the end of the Scheil solidification, 1313.4 °C. The nucleation of the γ'-phase takes place in presence of about 28.6 pct of liquid phase. According to the Scheil calculations shown in Figure 3(a), the nucleation of primary γ' results in an abrupt decrease in the liquid amount and an abrupt increase in the γ-matrix phase. After this abrupt change, the solidification ends with a smooth change of phase fractions as function of temperature.

Since, according to Scheil, the precipitation of the γ' is a primary transformation, a simile can be made with respect to the as-cast microstructure and it can be assumed that this primary γ' is part of the eutectic regions that form at the end of the solidification process. On the other hand, it can be assumed that part of the 28.6 pct of the remaining liquid present at the time of γ' nucleation will contribute to the formation of the eutectic regions. Table VI lists the chemical composition of the last 28.6 pct of the liquid phase during Scheil solidification, which can be assumed to be responsible for the generation of the eutectic regions during further solidification. The last 28.6 pct of the liquid contains a large amount of γ'-forming elements, Al, Ti and Ta and a low amount of the refractory and heavy elements Re and W, which agrees with what was experimentally measured in the eutectic regions of the as-cast material (Table IV).

Figure 3(b) shows the property diagram, where the molar fractions of the phases are plotted against the temperature, calculated under equilibrium conditions for the CMSX-10 K superalloy. The diagram shows that solidification starts at 1438.4 °C (liquidus temperature) with the γ phase and solidification ends at 1391.5 °C (solidus temperature). At 1369.3 °C, the γ'-phase appears through a solid–solid transformation and reaches a phase fraction of about 70.5 pct at 760 °C, which is the temperature of the last step of the aging heat treatment required to establish the correct γ/γ' microstructure[7,25,26]). At temperatures below 1098 °C, the presence of the Chi_A12 (χ) phase is calculated, the maximum amount of which does not exceed 1.2 mol fraction pct at 760 °C.

Due to the strong segregation of the as-cast material, the melting temperature associated with the eutectic regions measured by DSC, 1361 °C, differs considerably from the 1391.5 °C calculated by Thermo-Calc® software for the solidus temperature corresponding to the alloy composition under equilibrium conditions [Table V, Figure 3(b)]. To understand the effect of super-solidus heat treatments on the microstructure, temperatures of 1365 °C and 1370 °C, both slightly higher than the solidus temperature measured by DSC and published in Ref. 24, have been selected as maximum temperatures for these heat treatments. Thus, a fast heating rate of the as-cast CMSX-10 K material up to 1365 °C or to 1370 °C is expected to melt some

Table VI. Composition in Wt Pct of the Last 28.6 Pct of Liquid During Scheil Solidification, Reached at a Temperature of 1379.4 °C

	Ni	Cr	Mo	Co	W	Re	Al	Ti	Ta	Hf	Nb
28.6 pct liquid	bal	2.3	0.5	2.4	1.1	2.6	7.1	0.4	12.6	0.1	0.2

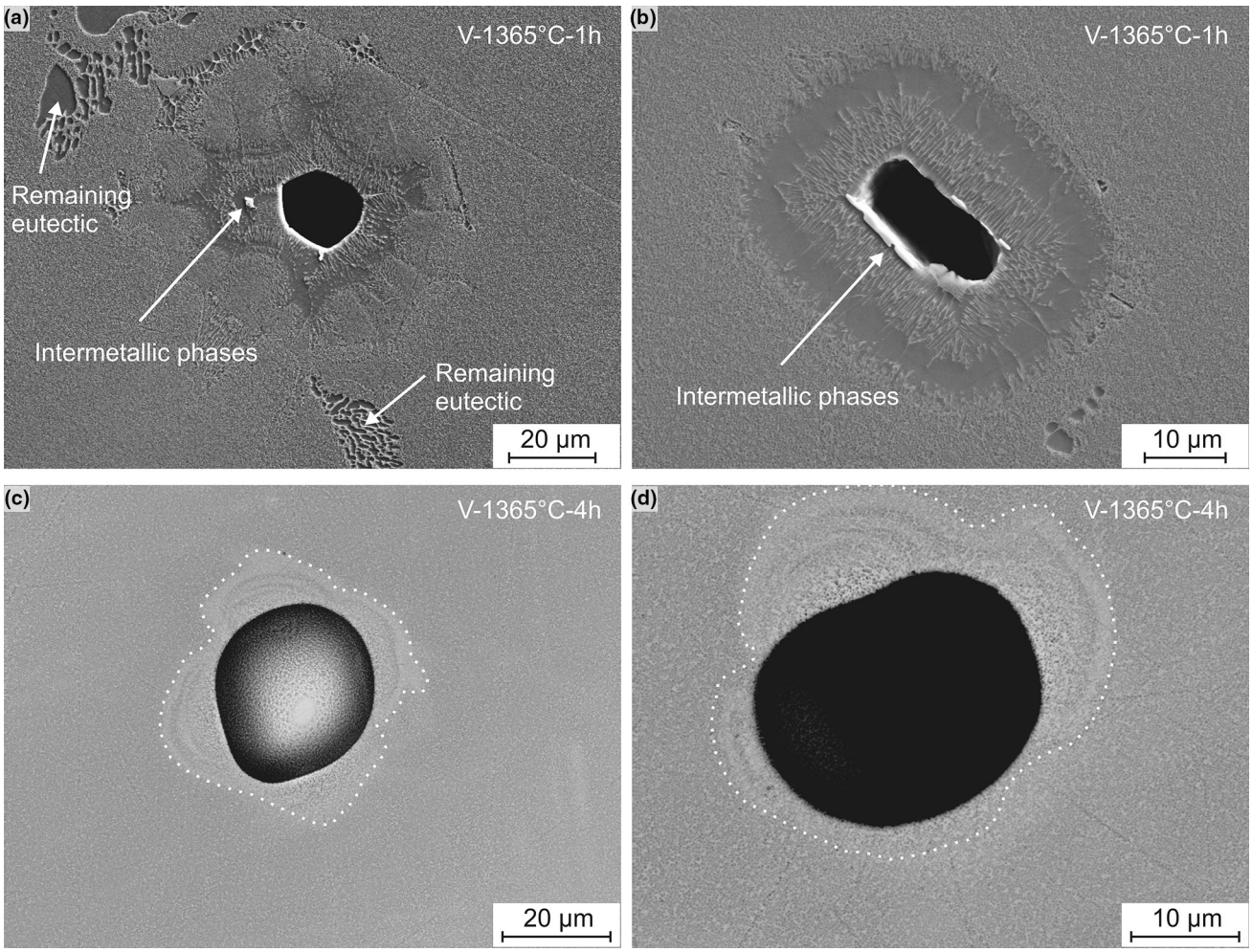

Fig. 4—Microstructures obtained at the interdendritic regions in the areas where the eutectic regions are or were placed, after a super-solidus heat treatment at 1365 °C for 1 hour, V-1365 °C-1 hour (*a* and *b*) and for 4 hours, V-1365 °C-4 hours (*c* and *d*). The specimens were heat-treated in a vacuum furnace. White arrows in (a) and (b) point the new generated intermetallic particles as well as remaining eutectic regions. White dashed lines in (c) and (d) mark the regions where monocrystalline re-solidification occurred.

eutectic regions, which have the lowest melting temperature, with adequate amount of melt to enhance diffusion processes, preserve the integrity of the specimens and improve their properties.

B. *Isothermal Super-Solidus Heat Treatments*

Figure 4 shows representative figures of the microstructures obtained in the specimens thermally treated in a vacuum furnace at 1365 °C for 1 hour and 4 hours of holding time, V-1365 °C-1 hour and V-1365 °C-4 hours respectively. A quantitative metallographic evaluation of the amount of porosity, of the remaining cast-eutectics as well as of the new re-solidified eutectic regions for these two specimens is listed in Table III. The application of 1 hour of holding time at the super-solidus temperature results in a partial melting of the eutectic areas, which mostly re-solidify in the same position from where they melted. In addition, a remaining amount of eutectic regions of about 1.89 area pct was measured. Figures 4(a) and (b) show representative re-solidified regions found in the V-1365 °C-1 hour specimen. Re-solidified regions, which represent 2.13 area pct of the material, contain

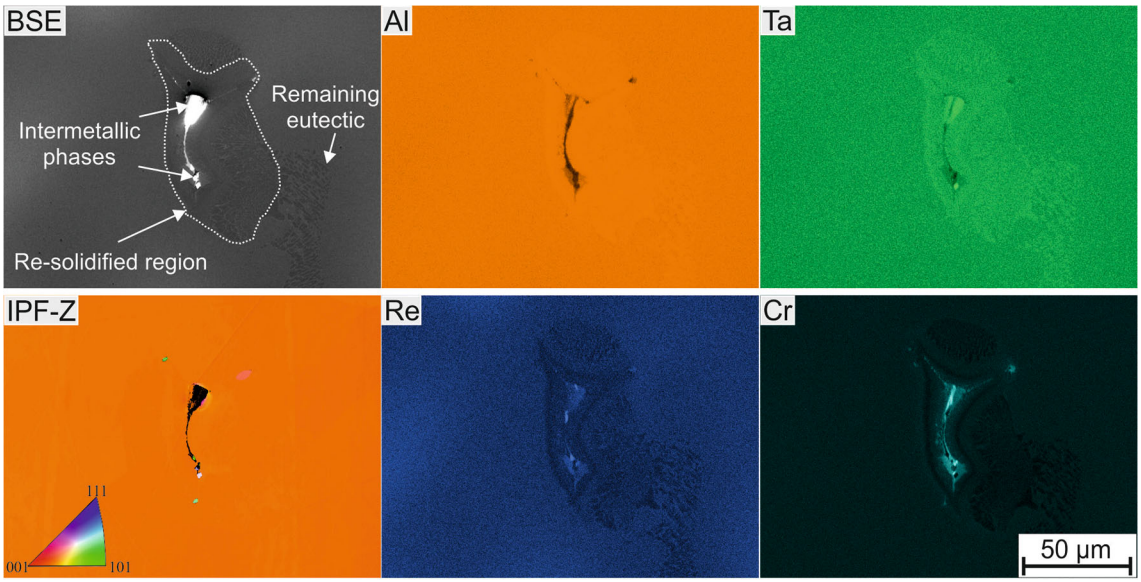

Fig. 5—Re-solidified region at V-1365 °C-1 hour. Inverse pole figure (IPF) obtained with a standard EBSD detector and chemical distribution of the elements throughout the re-solidified region. The concentration maps measured by EDX of the elements Al, Ta, Re and Cr are shown (Color figure online).

a relatively high amount of undesired intermetallic precipitates and have large pores that are trapped within the re-solidified material, 0.21 area pct of porosity. Figure 5 shows qualitative concentration maps for the alloying elements Al, Ta, Re and Cr measured in one of the re-solidified regions, also shown in Figure 5. It can be seen that the re-solidified regions are enriched with the γ'-forming elements Al and Ta, while they contain lower amount of the heavy elements Re and W (not shown). The intermetallic particles found in the centre of the re-solidified regions contain high amount of Cr, Re, Hf and W. The identification of the nature of these intermetallic phases has not been addressed in this work because it aims to develop a SSHIP heat treatment that prevents any of these unwanted phases. However, the high content of Cr, Re, Hf and W in these phases indicates that they could be the μ-phase, the σ-phase or a type of Laves phase.[35]

The most interesting aspect of the presence of re-solidified regions is knowing their orientation, which is the key point to know if the monocrystalline nature of the CMSX-10 K material has been preserved. Figure 5 shows the inverse pole figure (IPF) measured in a re-solidified region using a standard EBSD detector. It can be concluded that the molten material re-solidified with the same orientation as the parent material, which means that the generation of new grains did not occur and therefore the material maintained its monocrystalline nature.

A longer holding time of 4 hours at 1365 °C under vacuum conditions (specimen V-1365 °C-4 hours) results in better homogenization of the alloy composition between DC and ID, and greater dissolution of the eutectic regions, although some remnants of cast-eutectic regions were still visible, which represent 0.16 area pct of the material. In addition, a very low amount of very small re-solidified regions, which represent 1.31 area pct of the material, containing some intermetallic phases were observed, of the same type as those described for the V-1365 °C-1 hour specimen and shown in Figures 4(a) and (b). Finally, in specimen V-1365 °C-4 hours, a large amount of pores, 0.27 area pct, was found around which re-solidified material resides. The large amount of pores is related to the expansion of the material originating from the liquid formation at super-solidus temperatures and its subsequent shrinkage during cooling, Figures 4(c) and (d).

The RVB-EBSD characterization of the misorientations in the re-solidified regions around pores is shown in Figure 6. The left column of Figure 6 shows a forward scattered electron (FSE) map representing a superposition of orientation and chemical contrast. It can be seen that the crystal shows some slight inhomogeneities and misorientations adjacent to the pores. The <001> pole figure colour coding in the second column of Figure 6 shows that the pores nucleate directly on a low angle grain boundary (LAGB) separating two dendrites (-d1-/-d2- and -D1-/-D2- respectively). The misorientation angle between the dendrites -d1- and -d2- (specimen V-1365 °C-1 hour) was determined to 1.68 deg and between dendrites -D1- and -D2- (specimen V-1365 °C-4 hours) to 0.27 deg, respectively. Slight colour variations along the outer edge of the pores hint to local misorientations, which become more visible in the misorientation to mean orientation (Mis2Mean) mappings in the third column of Figure 6. The line profile along L1 shows that the local misorientations are in the order of 4 deg and expand over a maximum width of about 10 μm after a heat treatment of 1 hour at 1365 °C (upper row of Figure 6). These local misorientations are caused by elastic and plastic deformations of the crystal. The right

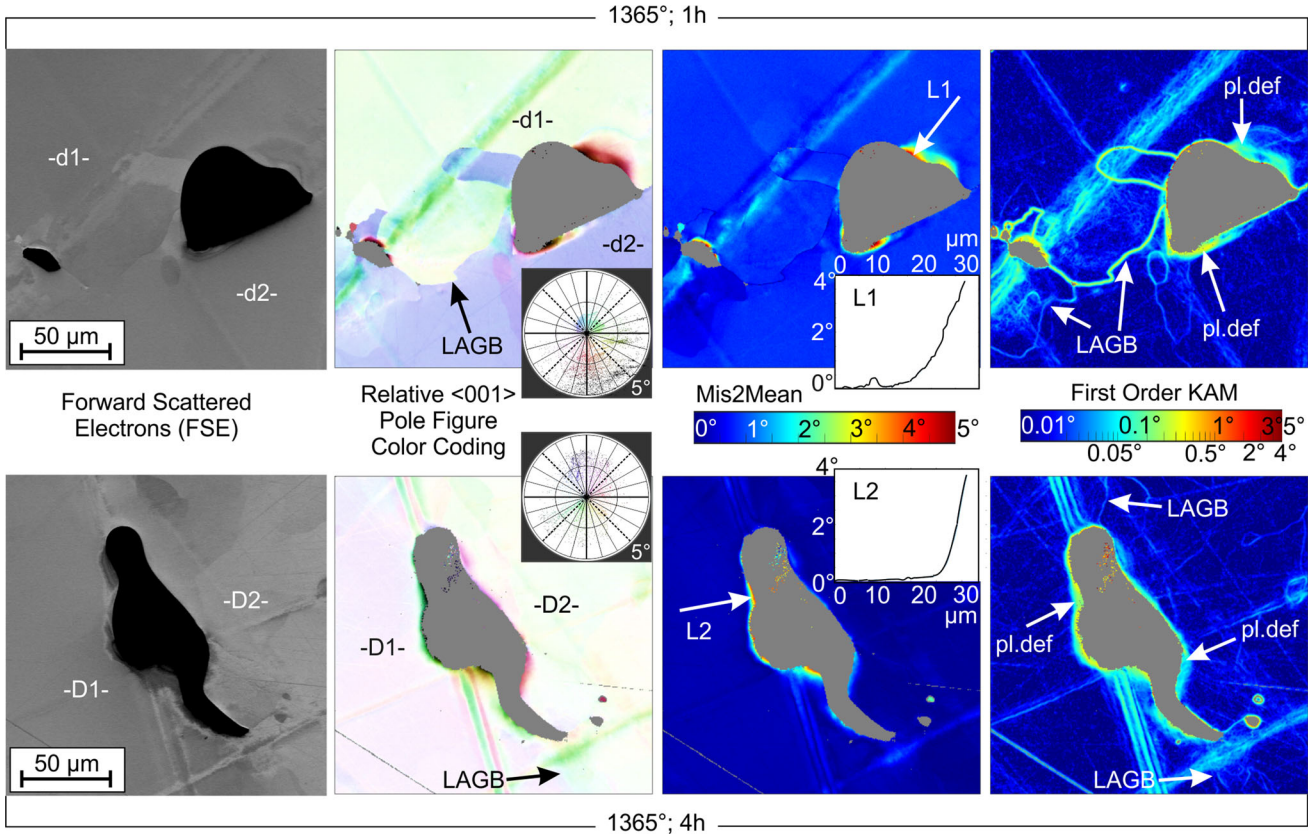

Fig. 6—RVB-EBSD characterization of the re-solidified regions around pores. Upper row: Heat treatment at 1365 °C for 1 hour, V-1365 °C-1 hour specimen; Lower row: Heat treatment at 1365 °C for 4 hours, V-1365 °C-4 hours specimen. Columns from left to right: (1) forward scattered electrons (FSE); (2) relative orientation mapping with <001> pole figure colour coding (max. angle: 5 deg); (3) misorientation to mean orientation (Mis2Mean) mapping; (4) first order kernel average misorientation (KAM) mapping (Color figure online).

column of Figure 6 visualizes a first-order kernel average misorientation (KAM) mapping (step size: 0.5 μm). The KAM mapping reveals both LAGBs as well as regions of plastic deformation (pl.def.). It can be seen that around the pore (Figure 6, upper row, right column) there is a region with maximum KAM values of about 0.5 deg and a width of approximately 10 μm indicating plastic deformation in the surrounding of the pore.

Comparing the RVB-EBSD Mis2Mean and KAM mappings (Figure 6, third and fourth column) of the 4 hours heat-treated sample (lower row, Figure 6) at 1365 °C with the 1 hour heat-treated sample (upper row, Figure 6) shows similar crystallographic characteristics. However, it can be seen that after 4 hours heat treatment the extent of the local misorientations around the pore has been reduced in dimensions. The line profile across L2 shows that the absolute magnitude of the local misorientation is in a similar order as observed in the 1 hour heat-treated sample (approximately 4 deg), but the width of the misoriented region is now smaller than 5 μm. The KAM mapping in Figure 6 (lower row, right column) also reveals a region of plastic deformation around the pore after 4 hours heat treatment at 1365 °C. The width of this deformation zone is significantly smaller (< 5 μm) than in the 1 hour heat-treated sample.

The results explained above suggest that a longer heat treatment at super-solvus temperature is necessary for the complete dissolution of eutectic regions and to avoid the presence of re-solidified regions with unwanted intermetallic phases. However, heat treatments with longer holding times are associated with an increase in porosity and thus a consequent reduction in mechanical properties.[9,12,13] In order to avoid the formation of new porosity, super-solidus heat treatments under isostatic pressure have been studied in this regard. The isostatic pressure applied was in all cases 100 MPa and after the holding stage at the maximum temperature, a rapid cooling rate was applied. The isothermal HIP heat treatments were carried out for 4 hours at 1365 °C, HIP-1365 °C-4 hours, and for 4 hours at 1370 °C, HIP-1370 °C-4 hours, in order to study the effect of increasing the maximum temperature by 5 °C, while keeping the maximum holding time at 4 hours.

The super-solidus HIP heat treatment at 1365 °C for 4 hours resulted in dense specimens with a remaining fraction of eutectics of about 5 area pct. At the interdendritic regions the presence of new re-solidified areas or formation of intermetallic phases was not observed [Figure 7(a)]. However, increasing the temperature by 5 °C results in the complete dissolution of the cast-eutectics, but, conversely, the presence of few regions containing re-solidified structures (0.20 area

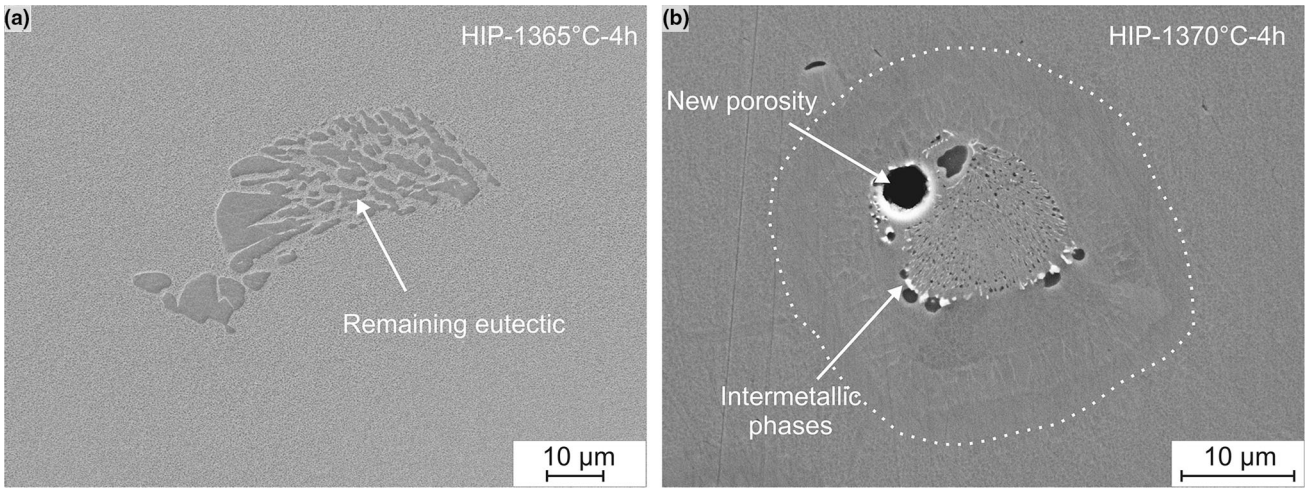

Fig. 7—Microstructures obtained at the interdendritic regions in the areas where the eutectic regions are or were placed, after a HIP super-solidus heat treatment at 1365 °C for 4 hours, HIP-1365 °C-4 hours (*a*) and at 1370 °C for 4 hours, HIP-1370 °C-4 hours (*b*).

pct), intermetallic precipitates and small pores (0.05 area pct) [Figure 7(b)]. In those regions where these defects did not occur, the eutectic regions completely dissolved and no remaining porosity was observed. Here again, this highlights the importance of controlling the temperature of the heat treatments.

C. *SSHIP*

The microstructural characterization of the specimens subjected to the SSHIP heat treatment allows to conclude that the SSHIP yields the completely dissolution of the eutectic regions (< 0.1 area pct of remaining eutectics), the porosity closure (< 0.002 area pct of porosity) and avoids the presence of new re-solidified regions and the formation of brittle intermetallic phases. The total holding time of 10 hours at super-solidus temperature results in a high homogenization of the chemical composition between DC and ID regions. Concentration profiles measured by EDX for the elements Al, Ta, Re and W between DC and ID regions are plotted in Figure 8. The chemical compositions measured at the DC and ID are listed in Table IV. Here, the fastest diffusing alloying element Al is almost completely homogenized between the two regions mentioned, in the same way as the alloying element Ta. A strong reduction in segregation is measured for the two heaviest elements Re and W that have the lowest diffusion coefficients in nickel.

The good homogenization of the chemical composition presented in the SSHIP materials together with the fact that this material does not have remaining eutectic regions result in a single melting peak during the heating ramp of the DSC test [dashed line in Figure 2(a)], where the solidus temperature is measured at 1389 °C. This value is very close to the value of solidus temperature calculated by Thermo-Calc®, 1391.5 °C, for the case of equilibrium conditions, which indicates that the degree of chemical homogenization in the material has reached a high level. The liquidus temperature derived from the cooling signal of the DSC measurement [dashed line in Figure 2(b)] has a value of 1421 °C which is approximately equal to the measured for the as-cast material [solid line in Figure 2(b)]. This value is approximately 17 °C lower than that calculated with Thermo-Calc®, 1438.4 °C (Table V). From the DSC measurements performed, the exact temperature of γ'-solvus could not be measured; however, a small deviation of the DSC heating curve [dashed line in Figure 2(a)] from the horizontal line at 1344 °C (small and wide exothermic peak), could indicate that the γ' solvus occurs between approximately 1344 °C and 1367 °C, with the latter value very close to the γ'-solvus value calculated by Thermo-Calc® at equilibrium conditions, 1369.3 °C.

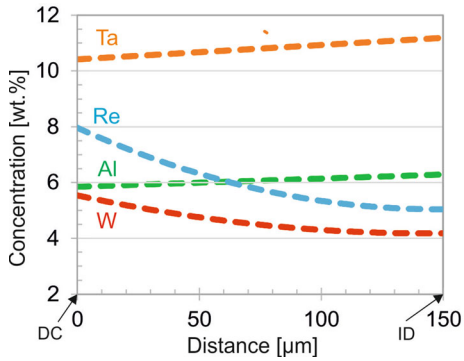

Fig. 8—Average EDX concentration profiles after the SSHIP between dendrite core (left side) and interdendritic regions (right side) for the selected alloying elements Al (green), Ta (orange), Re (blue) and W (red) (Color figure online).

D. *Mechanical Testing*

Two creep tests (temperature 1050 °C, stress level 170 MPa) were carried out for [001] single crystal CMSX-10 K specimens subjected to the developed SSHIP heat treatment and to a conventional aging heat treatment. The creep curves obtained in the present work and represented in Figure 9 show that both specimens

ruptured after more than 400 hours, a longer time than the 380 hours obtained by *Portella and Link*[34] under similar conditions (1050 °C, 180 MPa) for a CMSX-10 K with a 45 hours homogenization heat treatment.

Figure 10 shows representative micrographs of the developed microstructure during the creep test. After creep rupture, a topological inversion of the phases is observed where γ'-phase is interconnected and unconnected segments of the γ phase are embedded within the γ'-phase. In the crept specimens, a large number of creep pores were also observed (0.96 area pct), mainly with a rectangular geometry and connected with cracks. Finally, the long time to creep rupture experienced for the SSHIP specimens resulted in the development of needle-like intermetallic phases, Figures 10(d) and (e).

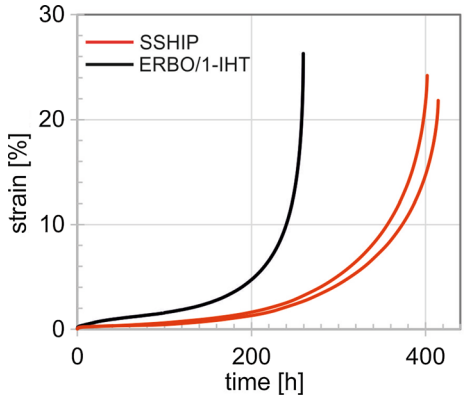

Fig. 9—Creep curves, strain *vs* time obtained at the creep conditions of 1050 °C and 170 MPa for two CMSX-10 K specimens heat-treated according to the designed SSHIP heat treatment (red lines). The creep results of the ERBO/1-IHT alloy obtained under creep conditions of 1050 °C and 160 MPa are included for comparison purposes (black line) (Color figure online).

IV. DISCUSSION

The as-cast microstructures of advanced SX Ni-base superalloys show strong chemical segregation within the dendritic structure in addition to other heterogeneities like high amount of γ/γ' eutectics, porosity or TCP phases. Because of these microstructural features, these materials require very long conventional homogenization-solution heat treatments at very high temperature,[1,7,24–26] which is why in many cases they are no longer attractive for the aeronautical sector despite their potential. Thus, any advance in the design of heat treatments that allows properties to be maintained or even improved while minimizing the heat treatment time can be of vital interest to the aeronautical sector. With that idea, the *super-solidus hot isostatic pressing* (SSHIP) heat treatment was developed. In the following, it is discussed how the SSHIP treatment works for SX Ni-base superalloys and what its benefits compared to

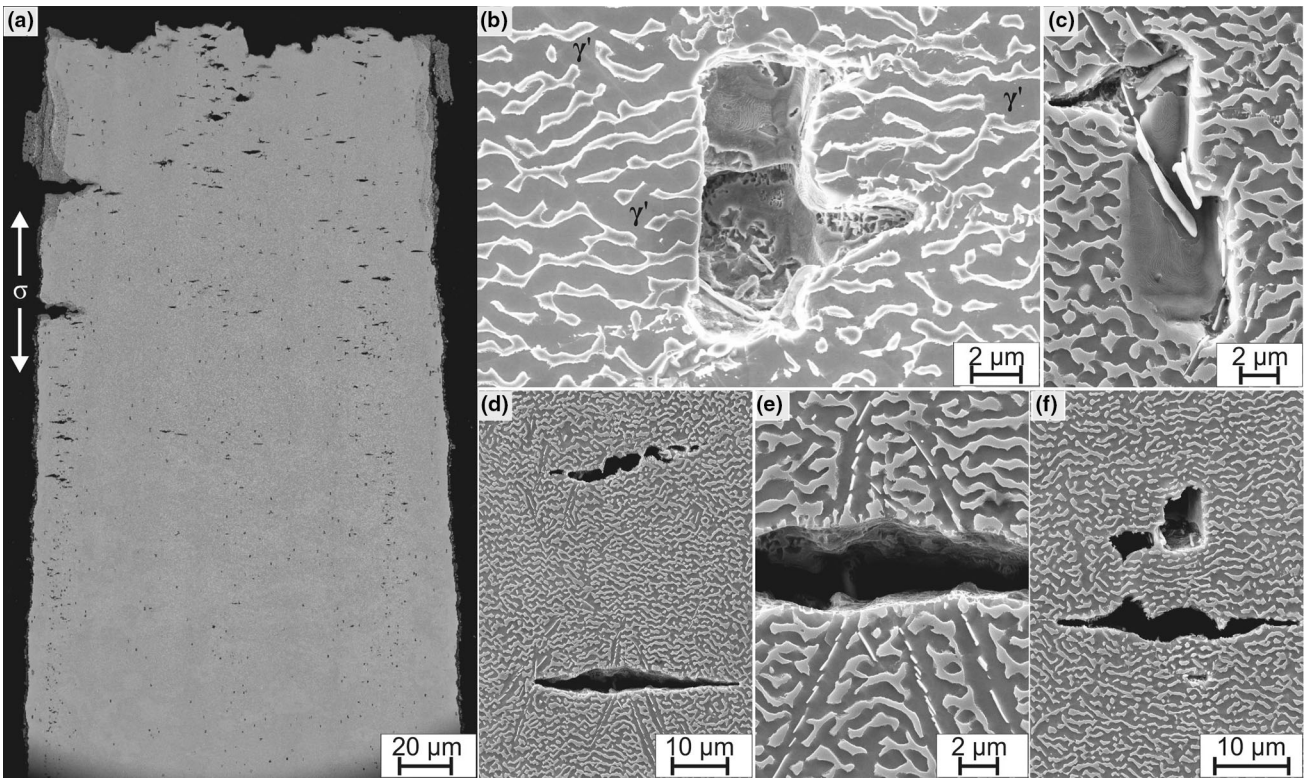

Fig. 10—Microstructures obtained after the creep tests carried out until rupture: (*a*) cross section of one half of the tested specimen; (*b*) topological inversion of the microstructure and creep pore with rectangular geometry and with a crack; (*c*) creep pore with rectangular geometry and with the presence of intermetallic phases; (*d–f*) cracks and intermetallic phases.

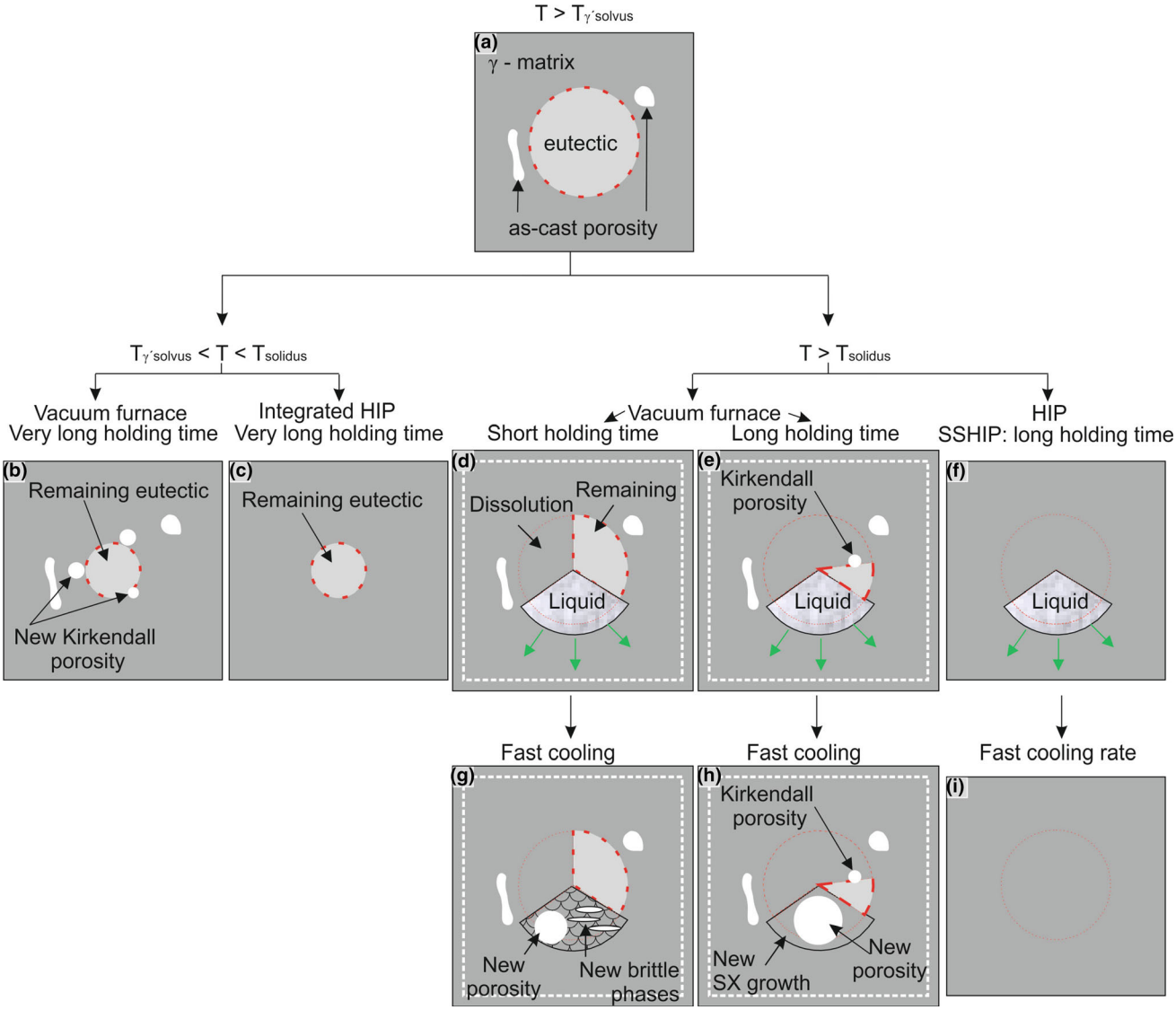

Fig. 11—Sketch of the evolution of the microstructure at the interdendritic regions when the as-cast material (*a*) is subjected to different heat treatment strategies; (*b*) standard solution annealing heat treatment; (*c*) integrated HIP heat treatment; (*d*) and (*g*) short super-solidus heat treatment in a vacuum furnace; (*e*) and (*h*) long super-solidus heat treatment in a vacuum furnace; (*f*) and (*i*) SSHIP heat treatment within a HIP unit. Dotted red lines indicate the initial and final perimeter of the eutectic phase. Dotted white lines indicate the initial volume of the study material. Green arrows indicate the volume expansion due to the melting of the eutectic regions, which lead to the expansion of the total volume of the material (Color figure online).

conventional heat treatments or even to the successful integrated HIP heat treatment are.[9,10,12,13]

A. *Main Differences Between SSHIP and Other Proposed Homogenization-Solution Heat Treatments for SX Ni Base Superalloys*

An adequate solution heat treatment, that is intended to be carried out with a reasonable duration, requires high temperature values. Conventional homogenization-solution heat treatments try to avoid exceeding the solidus temperature but nevertheless do reach the γ'-solvus temperature to facilitate diffusion processes within the γ-matrix. Therefore, any as-cast segregated SX microstructure subjected to a heat treatment at temperature above γ'-solvus ($T > T_{\gamma'\text{-solvus}}$), for a short holding time, develops a microstructure consisting basically of the γ-matrix phase, the as-cast porosity and the non-equilibrium eutectic regions, as shown schematically in Figure 11(a). Starting from this initial microstructure different heat treatment strategies can be proposed.

The application of the conservative—conventional solution heat treatment basically consists of subjecting the material to the highest possible temperature but always below the melting temperature so that over time (long time) the dissolution of the eutectics is achieved and segregation is reduced, Figure 11(b). Due to the fact that the diffusion processes of the alloying elements Re and W, present in these monocrystalline materials, are extremely slow (see Figure 12), the times required to have an acceptable chemical homogenization are

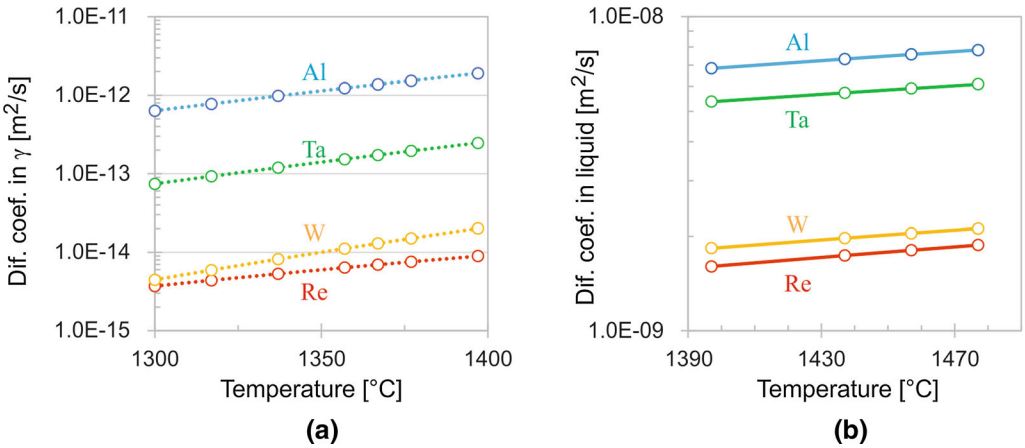

Fig. 12—Chemical diffusion coefficients of the allowing elements Al, Ta, Re and W in the γ-phase (*a*) and in the liquid phase (*b*) as a function of the temperature. Values calculated with Thermo-Calc® (Color figure online).

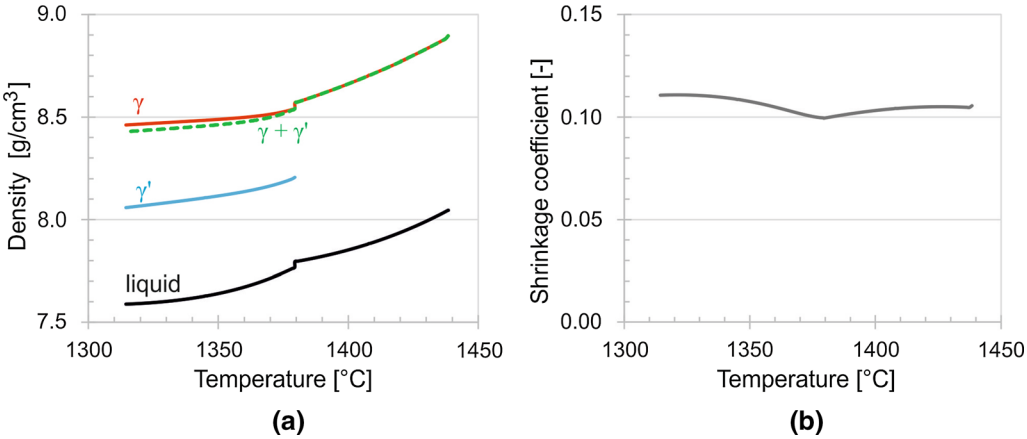

Fig. 13—(*a*) Density of the phases as a function of temperature during the Scheil solidification; (*b*) shrinkage coefficient of the liquid phase during solidification, calculated according to Eq. [2] (Color figure online).

extremely long, and this justifies the extremely long heat treatments developed for the CMSX-10 superalloy.[1,7,24–26] The long conventional solution heat treatment is associated with an increase in porosity content due to the Kirkendall effect.[8] Furthermore, small amounts of eutectic regions are commonly found in fully heat-treated alloys. These microstructural characteristics resulting from the application of conventional heat treatments are schematically presented in Figure 11(c), which consists of carrying out the conventional solution heat treatment within a HIP unit, does not entail any significant reduction in the total treatment time. This is because the maximum temperatures used in the IHT heat treatment are the same as those defined in the conventional treatment and therefore long periods of time are needed to achieve chemical homogeneity. Thus, the application of IHT treatment can result in microstructures with small amounts of eutectic regions. The greatest benefit of the application of this treatment is the total reduction of porosity, both the as-cast porosity and that developed through the Kirkendall effect. On the other hand, a second benefit associated with the IHT treatment is the possibility of applying rapid cooling (only in modern HIP Units), resulting in very fine γ/γ' microstructures, which improve the mechanical properties.[9,10,12,13]

Reducing the total solution and homogenization heat treatment time while reaching a certain degree of homogenization can only be achieved by increasing the heat treatment temperature. Performing the solution heat treatment at temperatures slightly above the local solidus temperature results in the melting of regions with the lowest melting temperature, commonly associated with non-equilibrium eutectic regions. Due to the lower density of the liquid phase generated with respect to the density of the surrounding material, an expansion of the material (the γ-matrix) occurs by plastic deformation. Figure 13(a) shows the evolution of the phase density values as a function of temperature during Scheil solidification, calculated using the Thermo-Calc® software. The density of the liquid phase is approximately 0.8 g/cm^3 lower than that calculated for the solid phases,

regardless of whether this phase is only the γ-matrix or the combination of both solid phases, γ and γ'.

Considering that the material to be heat-treated has the microstructure depicted in Figure 11(a), where the eutectic regions and the as-cast porosity are embedded in a γ-matrix, the application of a heat treatment at temperatures slightly above solidus in a vacuum furnace or at atmospheric pressure has different effects on the microstructure depending on the duration of the heat treatment. When a short ($\leq$ 1 hour) super-solidus heat treatment is applied, Figure 11(d), it is considered that a part of the eutectic region dissolves, a part of the eutectic region remains because it has a solvus temperature value higher than the applied temperature, and a part of the eutectic region melts due to the applied super-solidus temperature. The melting is associated with an expansion of the total volume of the material [represented with green arrows in Figure 11(d)]. Due to the short duration of the holding time, diffusion processes hardly have time to occur to make a relevant change in the degree of homogenization of the material. Therefore, the application of a subsequent fast cooling results in the re-solidification of the molten material at the same region where it was generated. Due to different partitioning coefficients, intermetallic phases can be found at the new re-solidified regions, and due to the shrinkage of the liquid phase, new porosity is generated at the re-solidified regions. The microstructural characteristics resulting from the application of a short super-solidus heat treatment are shown in Figures 4(a) and (b) and schematically presented in Figure 11(g). From the RVB-EBSD characterization of the re-solidified regions around pores, it can be concluded that the shrinkage of the re-solidified regions causes zones with plastic deformations around the new pores, Figure 6 (right column).

The application of longer super-solidus heat treatments ($\geq$ 4 hours), Figure 11(e), does not necessarily result in the formation of higher amount of molten regions; however, a higher amount of eutectic regions dissolves and therefore, a lower amount of remaining eutectics is expected. Furthermore, longer holding times at the super-solidus temperature allow solid–solid diffusion processes, as well as liquid–liquid diffusion processes, to take place more effectively, reducing the level of segregation through the material and generating homogenization porosity (Kirkendall effect). Figure 12 shows the chemical diffusion coefficients of selected alloying elements, Al, Ta, W and Re, in the γ-matrix FCC_L12 and in the liquid phases as a function of temperature. Diffusion coefficients in the liquid phase are more than 3 orders of magnitude larger than in the solid γ-phase, therefore, from the point of view of material homogenization, the formation of molten regions is considered beneficial. During these diffusional processing, compositions of liquid and the regions around liquid change, producing a partial solidification of the liquid. The partial solidification during longer heat treatments and the resulting better homogenization reduces the extent of plastic deformation around pores in the re-solidified regions, Figure 6 (right column). During fast cooling, the remaining liquid solidifies with an orientation that mimics that of neighbour materials. Therefore, the re-solidification of a single crystal is obtained, as shown in Figures 5 and 6. The microstructural characteristics resulting from the application of a long super-solidus heat treatment are schematically presented in Figure 11(h). The main drawback of this heat treatment is the large amount of porosity that is generated due to the initial expansion of the material and the final liquid shrinkage, Figures 4(c) and (d). This mechanism for porosity growth was not considered in previous studies,[11,36] but was described by Hegde *et al.*[37] The maximum volume of this new type of porosity generated during super-solidus homogenization-solution heat treatment seems to be proportional to the total volume of eutectics presented in the as-cast microstructure, since they are the regions that are likely to melt during these heat treatments. A correlation between the volume fraction of porosity generated by the previous described mechanisms at super-solidus temperature, $V_{\text{p- super-solidus}}$ and the non-equilibrium eutectics generated during the casting process, $V_{\text{Eutectic}}^{\text{as-cast}}$ can be described by the following equation:

$$V_{\text{p- super-solidus}} = \beta \cdot V_{\text{Eutectic}}^{\text{as-cast}} \quad [1]$$

where β is the volume shrinkage coefficient of the liquid during solidification which can be described as:

$$\beta = \frac{\rho S - \rho L}{\rho_{\text{L}}} \quad [2]$$

where ρ_{S} and ρ_{L} are the densities of the solid phase γ and the liquid phase, respectively. Figure 13(b) shows the values of the shrinkage coefficient of the liquid phase during solidification at high temperature, calculated according to Eq. [2]. These values range from 0.1 to 0.11 in the range of temperatures studied. Zhang *et al.*[38] published an experimentally measured value of 0.051 for the volume shrinkage coefficient. In order to know the maximum amount of porosity that can be generated due to the application of a super-solidus heat treatment, it can be considered that all the eutectics present in the as-cast material melt during the application of a super-solidus heat treatment. Considering an average value of 0.1 for the calculated shrinkage coefficient of the liquid phase during solidification [Figure 13(b)] and the initial value of 22 area pct of eutectic regions (value measured in the as-cast CMSX-10 K, Table III), the application of Eq. [1] results in a value of 2.2 area pct of porosity. This very high porosity value, which could adversely affect the mechanical properties, could be reached when the temperature chosen for the super-solidus heat treatment is extremely high, creating a large amount of liquid with consequent swelling of the material.

A reasonable way to reduce the total solution heat treatment time and avoid the adverse effect of the presence of porosity is to apply the SSHIP with an appropriate holding time to dissolve and melt the totality of the eutectic regions. The application of a SSHIP heat treatment, Figure 11(f), results in the

dissolution of a large area of eutectics and melting of the remainder with the related benefits discussed above in relation to the faster diffusion mechanisms associated with the presence of the liquid phase at super-solidus temperatures. The application of isostatic pressure during the annealing process annihilates the as-cast and homogenization porosity as well as reduces the effects of the material expansion and the effects of shrinkage of the last remaining liquid during cooling. Finally, the application of a fast cooling after SSHIP results on the one hand, in a dense material without defects (pores, eutectics and intermetallic phases), Figure 11(i), and on the other hand, in a fine and homogeneous γ/γ' microstructure.

B. *The Benefit and Potential of the SSHIP Heat Treatments*

In this work, the development of the SSHIP heat treatment was performed and applied for the first time to the SX CMSX-10 K superalloy, which has a very high content of refractory elements and an extremely segregated microstructure in the as-cast condition (Table I; Figure 1). This heat treatment intentionally melts certain areas of the monocrystalline material during the two holding steps at super-solidus temperatures that make it up: 4 hours at 1365 °C and 6 hours at 1370 °C. The combination of the experimental characterization technique, DSC, with the calculations made in equilibrium and Scheil using the CALPHAD approach, were key to defining the processing parameters of the SSHIP heat treatment. Adequate control of all heat treatment parameters—temperature, time, pressure and heating / cooling ramps—made it possible to obtain a dense and homogeneous material without defects.

The mechanical performance of the SSHIP heat-treated alloy under demanding creep conditions (1050 °C and 170 MPa) has been shown to be good or even better than the conventional heat-treated alloy with a total holding time at high temperature of 45 hours[34] compared to 10 hours used in the SSHIP heat treatment. A rupture creep time of 380 hours was reported in[34] for the conventional heat-treated alloy, while SSHIP specimens with 10 hours homogenization time ruptured after more than 400 hours. Although the 10 hours of holding time of the SSHIP heat treatment is much shorter than the 45 hours that the conventional heat treatment lasts,[1,7] the authors are confident that the SSHIP can be further optimized and shortened so that the CMSX-10 K superalloy can be considered attractive for the aeronautical sector. In a recent publication[39] it has been found that for the SX CMSX-4 Plus, which also contains a high amount of refractory elements and a high amount of eutectic regions in the as-cast state, the presence of a large amount of re-solidified regions, generated intentionally, were not detrimental in terms of mechanical properties (very high cycle fatigue tests were studied in[39]). Therefore, the optimization of the SSHIP has to point in the direction of slightly increasing the temperature to provoke a greater amount of liquid phase. In this way the chemical homogenization processes will be accelerated. In the event that the residual liquid phase cannot be properly solidified during the cooling process at the end of the SSHIP heat treatment, the presence of small amounts of re-solidified material is expected not to affect the mechanical behaviour of the material.[39] This is because the solidification of the last remaining liquid occurs through an epitaxial growth process of the material that adopts the orientation of the parent material, and therefore the monocrystalline nature of the alloy is preserved, as shown in Figures 5 and 6 and described by Hegde *et al*.[37]

In Figure 9 the creep result of the second-generation ERBO/1 (CMSX-4 type) fully processed under an IHT heat treatment under isostatic pressure, shows a creep life of about 260 hours. The IHT heat treatment parameters can be found in[12] and its application result in dense specimens, without defects and with a very fine and homogeneous γ/γ' microstructure, the latter derived from the rapid cooling rate applied during the end of the homogenization step. Then, it can be said that the two heat treatments, IHT and SSHIP, result in dense and defect-free materials, with the difference that the first one requires more heat treatment time while the second one requires higher temperatures. The better creep performance of the CMSX-10 K material shown in Figure 9, with respect to that of the ERBO/1 material, is mainly explained by the difference in chemical composition between the two superalloys considered. According to Erickson,[7] CMSX-10 has about a 3 to 5 times better creep rupture life than CMSX-4; however, this advantage ends at around 1100 °C, where the rupture strength of both allows is similar. In this work, the advantage in creep strength of CMSX-10 K SSHIP heat-treated is approximately 1.6 times the creep rupture life of the ERBO/1, thus considerably less than that found by Erickson.[7] The reason for this may be due to the fact that the creep tests were performed at 1050 °C, thus only 50 °C below the temperature at which the rupture strength of CMSX-10 begins to approach that of the CMSX-4.

Several authors made efforts to optimize the solution annealing heat treatment for the CMSX-10 superalloy, thus reducing the total holding time from 45 hours corresponding to the conventional heat treatment[1,7,25] to the 26.75 hours proposed by Pang *et al*.[24] or the 17 hours heat treatment proposed by Ohtani.[26] The SSHIP heat treatment developed in this work significantly reduces the heat treatment time up to 10 hours without negatively affecting the microstructure and final properties. Therefore, this new type of solution annealing heat treatment could be considered as a replacement for the previously developed tedious and lengthy solution annealing heat treatments.[1,7,24–26]

V. CONCLUSIONS

This work investigates the effect of *super-solidus liquid phase heat treatments* on the microstructure and mechanical properties of the third generation CMSX-10 K Ni-base superalloy. From the results shown, the following conclusions can be derived:

- During the application of the *super-solidus hot isostatic pressing,* SSHIP, heat treatment a partial melting of the eutectic microstructure takes place while diffusion accelerates due to the higher temperature used. The derived swelling, due to liquid formation and the associated generation of new porosity during the cooling and resolidification stage of the material, is prevented due to the simultaneous application of isostatic pressure.
- The liquid remaining at the end of the super-solidus heat treatment re-solidifies as SX with the same orientation as the surrounding material.
- A proper selection of the SSHIP parameters allows to obtain dense materials without defects, such as eutectics, resulting in enhanced mechanical properties. The keys to the success of this heat treatment are based, on the one hand, on controlling the amount of molten material at the super-solidus temperatures and, on the other hand, on controlling the cooling rate to prevent the formation of misoriented grains and TCP phases during the re-solidification process.
- The SSHIP is an innovative and sustainable approach that could be applied to all types of SX superalloys, but especially to those which have a high content of refractory elements and a large volume fraction of eutectic microstructure in the as-cast state.

ACKNOWLEDGMENTS

The authors acknowledge funding by the *Deutsche Forschungsgemeinschaft* (DFG) in the framework of the collaborative research center SFB/TR 103 through projects A1(DB), B7(PT) and T4 (ILG, LH, BR, WT). The authors acknowledge *Quintus Technologies AB* as well as the *Center for Interface-Dominated High Performance Materials*, ZGH, of the Ruhr-Universität Bochum for their technological support and scientific discussions.

FUNDING

Open Access funding enabled and organized by Projekt DEAL.

CONFLICT OF INTEREST

On behalf of all authors, the corresponding author states that there is no conflict of interest.

OPEN ACCESS

REFERENCES

1. G.L. Erickson: *JOM, TMS Warrendale, PA*, 1995, vol. 47(4), pp. 36–9.
2. G.E. Fuchs: *Mater. Sci. Eng. A*, 2001, vol. 300, pp. 52–60.
3. S.M. Seo, J.H. Lee, Y.S. Yoo, C.Y. Jo, H. Miyahara, and K. Ogi: *Metall. Mater. Trans. A*, 2011, vol. 42, pp. 3150–159.
4. S.R. Hegde, R.M. Kearsey, and J.C. Beddoes: *Mater. Sci. Eng. A*, 2010, vol. 527, pp. 5528–538.
5. W.J. Boettinger, U.R. Kattner, K.W. Moon, and J. Perepezko: *NIST Spec. Publ.*, 2006, vol. 2006(960), p. 15.
6. T. Khan, P. Caron, and C. Duret: The Development and Characterization of a High Performance Experimental Single Crystal Superalloy. Proceedings Superalloys (Fifth International Symposium) 1984, pp. 145–55.
7. G.L. Erickson: The Development application of CMSX(R)-10. Proceeding: Superalloys (International Superalloys Symposium), 1996, pp. 35–44.
8. A. Epishin, T. Link, I.L. Svetlov, G. Nolze, R. Salivan Neumann, and H. Lucas: *IJMR*, 2013, vol. 104, pp. 776–82.
9. B. Ruttert, C. Meid, L. Mujica Roncery, I. Lopez-Galilea, M. Bartsch, and W. Theisen: *Scr. Mater.*, 2018, vol. 155, pp. 139–43.
10. L.M. Bortoluci Ormastroni, I. Lopez-Galilea, J. Pistor, B. Ruttert, C. Körner, W. Theisen, P. Villechaise, F. Pedraza, and J. Cormier: *Addit. Manuf.*, 2022, vol. 54, p. 102759.
11. V.N. Toloraya, A.G. Zuev, and I.L. Svetlov: *Izv. Akad. Nauk SSSR, Met.*, 1991, vol. 5, pp. 70–6.
12. L. Mujica Roncery, I. Lopez-Galilea, B. Ruttert, D. Bürger, P. Wollgramm, G. Eggeler, and W. Theisen: *Adv. Eng. Mater.*, 2016, vol. 18, pp. 1381–387.
13. C. Meid, A. Dennstedt, M. Ramsperger, J. Pistor, B. Ruttert, I. Lopez-Galilea, W. Theisen, C. Körner, and M. Bartsch: *Scr. Mater.*, 2019, vol. 168, pp. 124–28.
14. H. Klingelhöffer, A. Epishin, and T. Link: *J. Mater. Test.*, 2009, vol. 51, pp. 291–94.
15. I. Lopez-Galilea, S. Huth, and W. Theisen: *MATEC Web Conf.*, 2014, vol. 14, p. 13009.
16. L. Mujica Roncery, I. Lopez-Galilea, B. Ruttert, S. Huth, and W. Theisen: *Mater. Des.*, 2016, vol. 97, pp. 544–52.
17. A.I. Epishin, T. Link, B. Fedelich, I.L. Svetlov, and E.R. Golubovskiy: *MATEC Web Conf.*, 2014, vol. 14, p. 08003.
18. L. Wang, F. Pyczak, J. Zhang, L.H. Lou, and R.F. Singer: *Mater. Sci. Eng. A*, 2012, vol. 532, pp. 487–92.
19. C. Panwisawas, H. Mathur, J.C. Gebelin, D. Putman, C.M.F. Rae, and R.C. Reed: *Acta Mater.*, 2013, vol. 61, pp. 51–66.
20. R.M. German, P. Suri, and S.J. Park: *J. Mater Sci.*, 2009, vol. 44, pp. 1–39.
21. M. Jeandin, J.L. Koutny, and Y. Bienvenu: *Powder Metall. J.*, 1983, vol. 26(1), pp. 17–22.
22. A. Röttger, S. Weber, and W. Theisen: *Mater. Sci. Eng. A*, 2012, vol. 532, pp. 511–21.
23. S. Brust, A. Röttger, J. Kimm, and W. Theisen: *Int. J. Powder Metall.*, 2018, vol. 54(1), pp. 25–31.
24. H.T. Pang, N. D'Souza, H. Dong, H.J. Stone, and C.M.F. Rae: *Metall. Mater. Trans. A*, 2016, vol. 47, pp. 889–906.
25. M.V. Acharya and G.E. Fuchs: *Mater. Sci. Eng. A*, 2004, vol. 381(1–2), pp. 143–53.

26. R. Ohtani, N. Tada, M. Shibata, and S. Taniyama: *Fatigue Fract. Eng. Mater. Struct.*, 2001, vol. 24, pp. 867–76.
27. P. Thome, S. Medghalchi, J. Frenzel, J. Schreuer, and G. Eggeler: *Ultramicroscopy*, 2019, vol. 206, p. 112817.
28. P. Hallensleben, F. Scholz, P. Thome, H. Schaar, I. Steinbach, G. Eggeler, and J. Frenzel: *Crystals*, 2019, vol. 9, p. 149.
29. F. Scholz, M. Cevik, P. Hallensleben, P. Thome, G. Eggeler, and J. Frenzel: *Materials*, 2021, vol. 14, p. 4904.
30. H. Benker: *Mathematik mit MATLAB*, Springer, Berlin, 2000.
31. R. Hielscher and H. Schaeben: *J. Appl. Cryst.*, 2008, vol. 41, pp. 1024–037.
32. F. Bachmann, R. Hielscher, and H. Schaeben: *Solid State Phenom.*, 2010, vol. 160, pp. 63–8.
33. P. Wollgramm, D. Bürger, A.B. Parsa, K. Neuking, and G. Eggeler: *Mater. High Temp.*, 2016, vol. 33(4–5), pp. 346–60.
34. P.D. Portella, and T. Link. *DFG-project number 5193782*, 1999–2004.
35. I. Lopez-Galilea, J. Koßmann, A. Kostka, R. Drautz, L. Mujica Roncery, T. Hammerschmidt, S. Huth, and W. Theisen: *J. Mater. Sci.*, 2016, vol. 51, pp. 2653–664.
36. D.L. Anton and A.F. Giamei: *Mater. Sci. Eng.*, 1985, vol. 76, pp. 173–80.
37. S.R. Hegde, R.M. Kearsey, and J.C. Beddoes: *Scr. Mater.*, 2007, vol. 57, pp. 837–40.
38. J. Zhang and R.F. Singer: *Acta Mater.*, 2002, vol. 50, pp. 1869–879.
39. L.M. Bortoluci Ormastroni, L. Mataveli Suave, A. Cervellon, P. Villechaise, and J. Cormier: *Int. J. Fatigue*, 2020, vol. 130, p. 105247.